

X-ray absorption of the mercury distribution in a commercial metal-halide lamp

Abstract. The radial temperature profile of a commercial metal-halide lamp and of lamps containing its individual components have been acquired using x-ray absorption (XRA) of the Hg density distribution. The temperature profiles were determined by combining the measured absorption of the spatially resolved Hg density with the wall temperature. The lamps studied were a commercial lamp, i.e. the Philips CDM-T 70 W/830; and identically shaped lamps containing NaI, DyI₃ and TII separately. It was found that the element Dy contracts the arc, Na broadens the arc while Tl causes the arc to have so-called 'shoulders'. Combined in the commercial lamp this lead to a wall-stabilised arc without the contraction and 'shoulders'. A reproducibility test with identical lamps was also made and showed that the error in the temperature profile is about 8 % for the absolute temperature and only 1.6% for the actual shape of the profile.



Figure 8.1: Colour separation in a metal-halide lamp burner. The lamp is burned vertically upright. See figure 1.1 for full colour.

8.1 Introduction

The metal-halide lamp [1] consists of a buffergas of Hg and a small amount of metal-halide additives. The metals generate a myriad of lines in the visible part of the spectrum which results in high luminous efficacy and colour rendering. The metals themselves have low vapour pressure and tend to attack the walls of the burner at high temperatures [2]. These problems are avoided by using metal-halide salts such as DyI_3 , TII and/or NaI. In the metal-halide lamp a mixture of such salts are used in order to obtain a good colour rendering index. Mixtures such as $(\text{NaI} + \text{ScI}_3)$, $(\text{NaI} + \text{TII} + \text{InI})$ or $(\text{NaI} + \text{TII} + \text{DyI}_3 + \text{HoI}_3 + \text{TmI}_3)$ are commonly used in metal-halide lamps. Due to the competition between diffusive and convective processes these additives are non-uniformly distributed over the lamp, which in a vertical burning position results in a undesirable segregation of colours [3], see figure 8.1.

It is currently beyond our capabilities to fully understand a commercial metal-halide lamp with its complex shape and chemistry. Therefore poly-diagnostic experiments [4–10] have been performed on a reference lamp with a simple geometry and chemistry [11]. This reference lamp contains only one salt, which makes it easier to model. It would, however, be interesting to investigate a commercial lamp, which contains a mixture of species.

In order to gain a better understanding of the temperature distribution of the commercial lamp, it is also necessary to study its individual components. Therefore three salt components that make up the commercial lamp, TII, NaI, DyI_3 have been placed in separate lamps and measured by x-ray absorption. All lamps contain the same dosage of Hg as a buffer-gas. X-ray absorption (XRA) [4] [12–14] was used to measure the distribution of Hg atoms. This is done by irradiating the lamp with x-rays and by detecting the absorption of the x-ray photons in the whole lamp-burner. A temperature profile at different axial

positions of the discharge can then be obtained by applying the ideal gas law combined with the wall temperature.

The experiment and data-handling was designed by Zhu [4] and has been extensively examined and improved [14]. The latter study only investigated the two reference lamps as described earlier, namely the pure Hg and the Hg with DyI₃ lamp. Now the method has been improved it is of interest to focus on the application of XRA on a variety of lamps, such as the commercial Philips CDM-T 70 W/830 lamp.

Several methods are available for the determination of the temperature distribution in a discharge. Optical methods such as the determination of spectral line profiles [15–17] yield good results, but are limited to the central region of the discharge. X-ray induced fluorescence measurement of the Hg density distribution [9] performed earlier can measure the entire lamp but does not have the required spatial resolution to deal with the steep temperature gradient near the wall. XRA, however, has the benefit of both high spatial resolution and the ability to measure the entire lamp. Previous XRA measurements were performed by Fohl *et al* [18] and Curry *et al* [19]. The temperature for the latter was calibrated using an optical technique to determine the axis temperature. Our approach is different in the sense that the obtained relative temperature field is calibrated with an absolute measurement of the wall temperature, by infrared pyrometry [4]. In this paper the wall temperature is based on previous measurements done at Philips Lighting on similar lamps.

This chapter is organized as follows. Section 8.2 describes briefly the data-analysis necessary to obtain the temperature of the arc. Section 8.3 describes the lamps used in the experiments and the experimental setup. Results from the experiments are presented and discussed in section 8.4. These results include temperature profiles for the commercial lamp and its individual components and a reproducibility study. Finally, section 8.5 offers conclusions.

8.2 Theory

The basic process of XRA is that due to the interaction with inner-shell electrons x-ray photons are removed from the beam. Since the density of the buffer gas Hg outranges that of the other species, the primary observable is the Hg density distribution n_{Hg} . Therefore we can use the ideal gas law $p = n_{Hg}kT$ to translate the n_{Hg} -field into a spatial temperature profile [19]. This profile is calibrated with a wall temperature measurement.

The x-ray absorption measurement of the Hg concentration in metal-halide lamps requires two images: one for the lamp on and the other for the lamp off. By taking the ratio of these images (see figure 8.2), the absorption of Hg is obtained for each line-of-sight, i.e. for each lateral position. The radial density profile can then be reconstructed by using an inversion procedure called Abel inversion [20] [21], where the radial density function is represented by the even-order polynomial function.

We have to correct for a variety of image-disturbing influences that are caused by each part of the setup before the the ratio of the on and off-images can be taken. The main

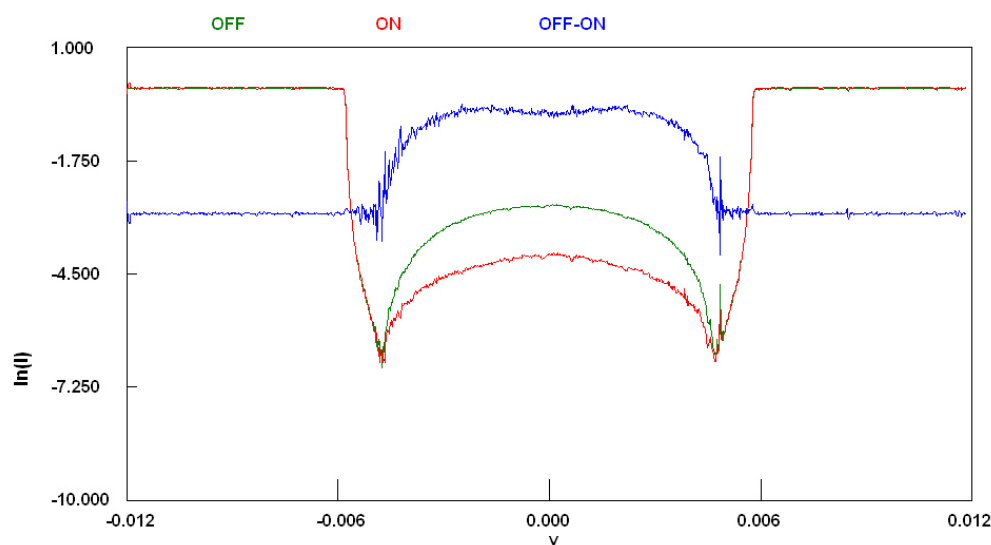


Figure 8.2: Lamp-on and off fitting of at one axial position, the difference between the fitted lamp-on and off profile, also shown, provides the absorption contribution of Hg. The line showing the difference between the on-and off profiles has been moved up by -3 and enlarged for clarity.

disturbing influences include the movement of the lamp during imaging, the blurring of the image caused by the finite dimension of the source and the scattering of the x-rays on the lamp materials. All disturbances are dealt with in the data-analysis procedure. The image disturbance and data-analysis has been studied extensively and reported in [4] [14].

8.3 Experimental setup

The setup, see figure 8.3, consists of three parts: the x-ray source for lamp irradiation, the lamp itself, and the CCD camera for imaging. A quasi-monochromatic x-ray beam generated by the Mo-anode x-ray tube, equipped with a Zr filter, is directed towards the metal-halide lamp under investigation, see figure 8.3. Part of the radiation will be absorbed while the remaining photons are detected by an x-ray CCD camera. CCD images are taken for two situations, a burning lamp (lamp on) and a non-burning lamp (lamp off). In the off-situation, the mercury is not present in the volume of the burner, but is condensed in small droplets on the wall or (usually) on the electrodes. When the lamp is burning, it is filled with mercury vapour. The mercury in the lamp-on situation causes an additional absorption of the x-ray photons. Therefore, the difference of the absorption signal between the lamp-on and lamp-off cases gives information on the mercury density [4]. It has been established that the vapour pressure of the salt-components are too low to contribute to the measurement of Hg. In the following sections we discuss the setup, consisting of a source and CCD camera, and the lamp used for the experiments.

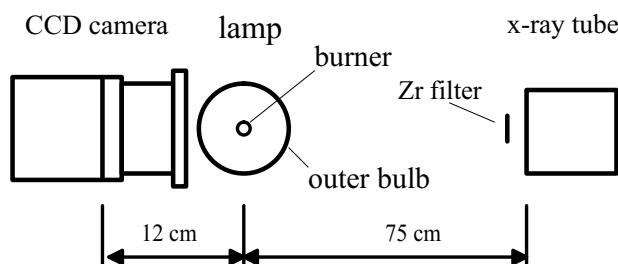


Figure 8.3: Top view of the x-ray absorption spectroscopy setup. The setup consists of a CCD camera, an x-ray tube and a lamp. The entire setup is encased in a box made of lead.

8.3.1 The lamp

The lamp consists of an 6.8 mm inner diameter PCA arc tube surrounded by a quartz outer bulb. The inner diameter of the outer bulb is 120 mm. The wall thickness of the burner is 0.55 mm. This is somewhat smaller than the 0.8 mm wall thickness that is used in the actual 70 W lamps on the market and were especially made for this experiment. A thin burner wall allows more x-rays to penetrate the area near the wall, dramatically improving signal-to-noise. The outer-bulb thickness is typically 1 mm. The inner length of the burner is 7 mm, as the electrodes do not protrude much above this, the electrode gap is therefore also approximately 7 mm.

Six different lamps were investigated, three pure Tl lamps containing 3.2, 5.6 and 8.0 mg TII; one DyI_3 lamp, one NaI lamp and finally a lamp containing a mixture of NaI, DyI_3 , TII, HoI_3 , TmI_3 . The latter is a commercial lamp mix, which is used in the Philips CDM-T 70 W/830. All lamps were built in the large quartz outer bulb for the experiment, see [14]. All six lamps contain 4.5 mg of Hg yielding a lamp pressure of about 30 bar. For the measurements presented here, the lamp was operated vertically at a power of 70 W. The power was supplied by an electronic square-wave ballast at a frequency of 122 Hz.

8.4 Results and Discussion

In order to gain a better understanding of the behaviour of the commercial lamp, both the individual chemical components were studied in individual lamps as was the commercial lamp itself, which is a mixture of these components. The components that are studied separately are DyI_3 , NaI, and TII. The commercial lamp contains these components plus the salts HoI_3 and TmI_3 but given the character of these rare earth components and their spectra it is expected that a DyI_3 lamp is representative for the $\text{DyI}_3/\text{HoI}_3/\text{TmI}_3$ mix.

The wall temperature is estimated to be 1350 K for these type of lamps. This temperature however is based on infrared pyrometry measurements done on a commercial lamp with a burner thickness of 0.8 mm. Because our lamps have a thinner burner thickness of 0.55 the wall temperature is estimated to be slightly higher and to be approximately 1400 K.

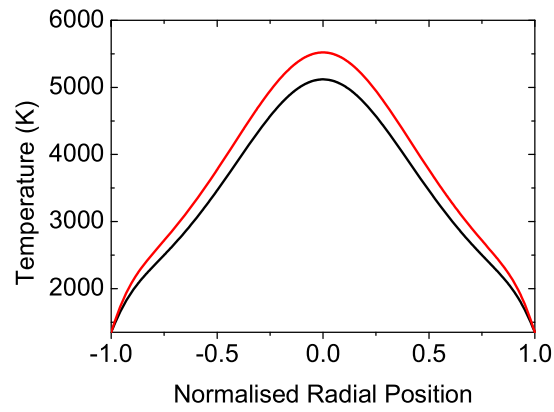


Figure 8.4: Radial temperature profiles at the midplane for two nominally identical lamps containing NaI and 4.5 mg Hg.

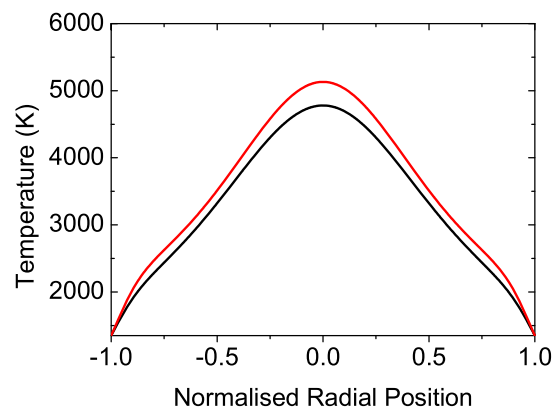


Figure 8.5: Radial temperature profiles at the midplane for two nominally identical commercial CDM-T 70 W/830 lamps.

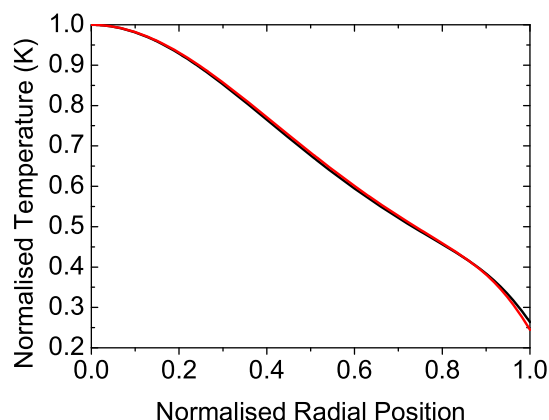


Figure 8.6: Normalised radial temperature profiles at the midplane for two nominally identical lamps containing NaI and 4.5 mg Hg.

In order to estimate the error of the temperature profiles two sets of identical lamps were measured, one set of two pure NaI lamps and the other of commercial lamps. The results of the radial temperature profiles are shown in the figures 8.4 and 8.5 for the NaI and the commercial lamps respectively. The axis temperatures show a difference of 8%, this is therefore assumed to be an indication of the error in the axis temperature. The error in the actual shape of the profile is studied by normalising the axis temperatures, see figures 8.6 and 8.7 for the NaI and commercial lamp. The difference between the temperature profiles are taken mid-radius and show that the error in shape is much smaller than the error in the axis temperature, namely 1.6%.

The radial temperature distribution of the mixture and the individual components were determined at the midplane and are shown in figure 8.8. In order to get a better view of each of the components the radial temperature profiles were normalised at the centre of the lamp, see figure 8.9.

The figure shows that Dy contracts the arc. The Dy spectrum consists of a myriad of optically thin lines. This means that most of the molecular and atomic radiation can escape the discharge which leads to cooling. Since this is mostly at the flanks, the arc contracts. The temperature of the pure DyI_3 lamp at the centre is about 4900. In contrast, Na has a spectrum that consists mainly of a few self-reversed resonance lines. The re-absorption of the Na lines occurs along the whole radius of the discharge, so the profile broadens as is shown in figure 8.9. The temperature at the centre of the pure NaI lamp is 5100 K. It is not possible to assess which of DyI_3 and NaI axis temperatures are actually higher given the limited accuracy of the experiment.

The results for a lamp containing 3.2 mg TII show that the temperature gradient at the wall is about twice as high for TII than for any of the other salts. Between 2500 and 3500 K the gradient sharply decreases thereby creating a 'shoulder'. The decrease in

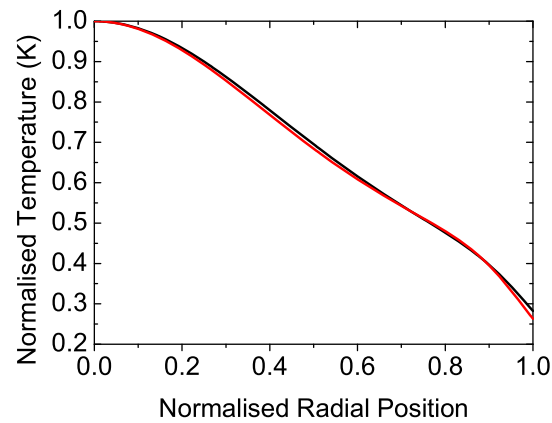


Figure 8.7: Normalised radial temperature profiles at the midplane for two nominally identical commercial CDM-T 70 W/830 lamps.

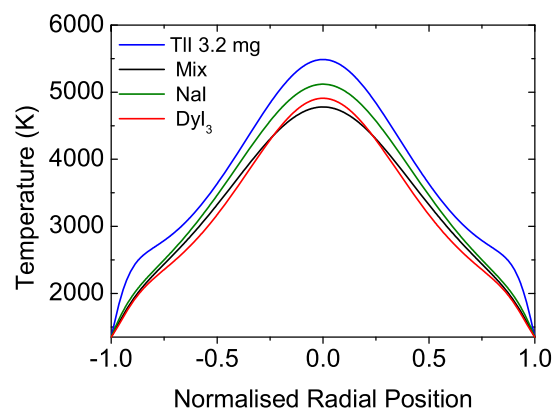


Figure 8.8: Radial temperature profiles at the midplane for lamps with 4 different fillings: pure NaI, pure DyI₃, pure Tl (3.2 mg) and a commercial CDM-T 70 W/830 lamp that contains a mixture of these, all lamps also contained 4.5 mg Hg. At the central radial position, the order of the profiles from the top is as follows, TII, NaI and DyI₃; the lowest profile is from the commercial lamp

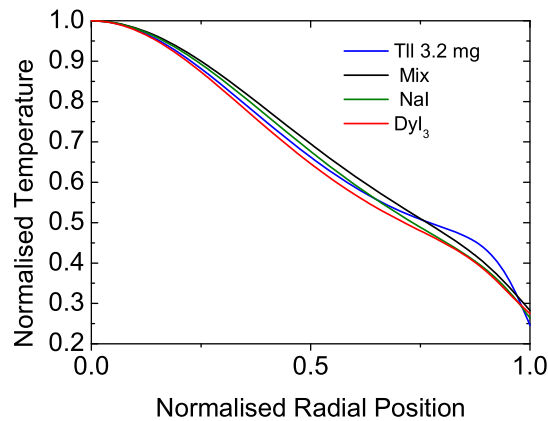


Figure 8.9: Normalised radial temperature profiles at the midplane of lamps with 4 different fillings: pure NaI, pure DyI₃, pure Tl (3.2 mg) and a commercial CDM-T 70 W/830 lamp that contains a mixture of these, all lamps also contained 4.5 mg Hg. At mid-radius, the order of the profiles from the top is as follows, the commercial lamp, the NaI, TII and DyI₃ lamps.

temperature gradient occurs in the temperature interval where the TII molecules dissociate into Tl atoms. Chemical calculations [22] show that the region where the equilibrium shifts from Tl molecules to Tl atoms is between 2000 and 4000 K, see figure 8.10. This shift is accompanied by the release of chemical enthalpy causing an increase in thermal conductivity [26], leading to the 'shoulder' in the temperature profile. This shoulder is not observed in the other pure salt-lamps because the vapour pressure is too low.

The commercial CDM-T 70 W/830, which consists of a mixture, combines the effects of the DyI₃ (and thereby of HoI₃ and TmI₃), NaI and TII which results in a non-constricted arc with a temperature at the centre of around 4800 K.

In contrast to DyI₃ and NaI, it is more likely for TII to evaporate completely in the lamp, so it is of interest to investigate lamps with different fillings. A total of three lamps with 8.0, 5.6 and 3.2 mg of TII were measured. The results are shown in figure 8.11. The profiles are determined at the midplane of the lamp. The average axis temperature for all three lamps is around 5500 K within the 8% error margin. To aid comparison the temperature profiles were normalised, see figure 8.12. The profiles are nearly identical, it is therefore of interest to find out how much Tl is actually in the discharge.

Emission spectra of the lamps containing Tl give insight in the amounts of Tl in the discharge. Four spectra of the three Tl lamps and the commercial lamp, containing the mixture, are shown in figure 8.13. The intensity is normalised at 535 nm. The line widths for the three different pure Tl lamps at 535 nm show that the amount of Tl in the discharge is comparable. This is consistent with the nearly identical temperature profiles of the three lamps. It is clear not all TII has entered the discharge. Apparently, in all cases the TII forms a saturated vapour at a similar cold-spot temperature in all three lamps. The spectra

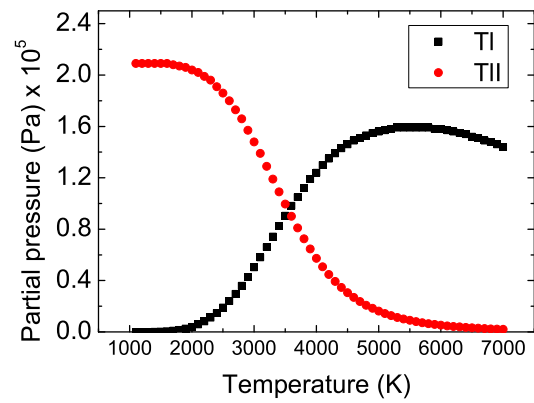


Figure 8.10: Chemical calculation [22] where 8 mg TII, 8 bar Hg, a lamp volume of 1 cm³ and a cold-spot temperature of 1100 K were assumed.

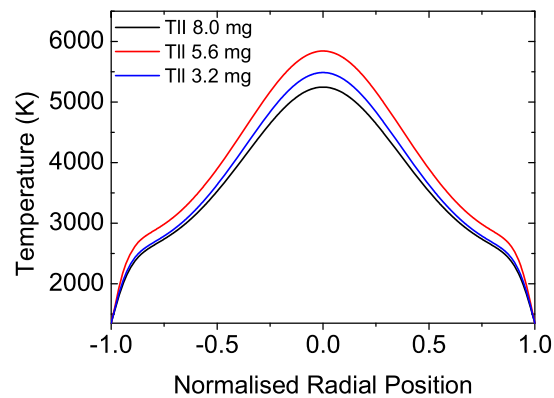


Figure 8.11: Radial temperature profiles at the midplane of lamps containing pure Tl and 4.5 mg Hg. At the central radial position, the TII filling is in the following order, 5.6 mg, 3.2 mg and 8.0 mg.

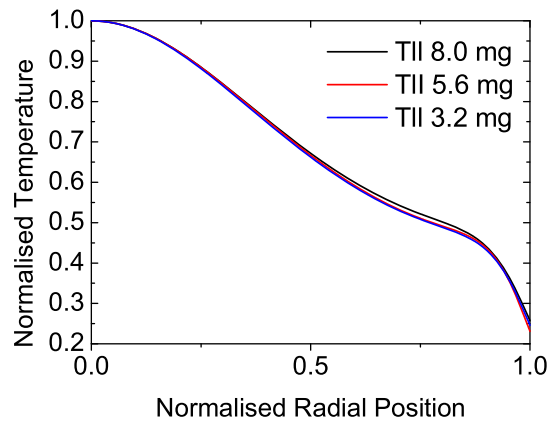


Figure 8.12: Normalised radial temperature profiles at the midplane for three different TII lamps containing 8.0, 5.6 and 3.2 mg of Tl and 4.5 mg of Hg. At mid-radius the order of the profiles is 8.0 mg, 5.6 mg and 3.2 mg.

also show that the vapour pressure of Tl in the commercial lamp is much lower than in the three pure Tl lamps. This explains why the shoulder of the Tl vapour is much less pronounced in the discharge containing the mixture.

Finally, a check of the validity of the experiments is made by the calculation of the absolute Hg density [4]. For this the x-ray absorption cross-section of $3.74 \cdot 10^{-24} \text{ m}^2$ [24] for the mean x-ray photon energy absorbed by the Hg at 17.6 keV is used. The density of the commercial lamp is shown in figure 8.14. It shows a density of $4.0 \cdot 10^{25} \text{ m}^{-3}$ at the centre and $1.4 \cdot 10^{26} \text{ m}^{-3}$ at the wall of the discharge. This leads to a pressure of 26 bar, this is consistent with the 30 bar of Hg in the lamp within the error margin, which is mainly related to the uncertainty of the cross-section and the effective x-ray energy.

8.5 Conclusions

The commercial metal-halide lamp temperature profile combines the effects of its various salt constituents. The metals in these lamps are mainly Dy, Na and Tl. Dy causes the profile to contract, whereas Na tends to broaden the profile, cancelling the contraction caused by the Dy. Tl has a pronounced effect on the shape of the temperature profile of a pure Tl lamp. The temperature profiles clearly show a region where the atoms associate into molecules and vice versa. This region has a sharply decreased temperature gradient and occurs between 2500 and 3500 K. The commercial lamp on the other hand has much less Tl in the discharge than the pure Tl lamps, causing the influence of Tl to be much less severe. The pure Tl lamps contain the same amount of Tl pressure, despite the fact that they have different fillings. The results are found to be reproducible for different identical lamps of the same filling, the error is axis temperature is found to be 8 % and for the

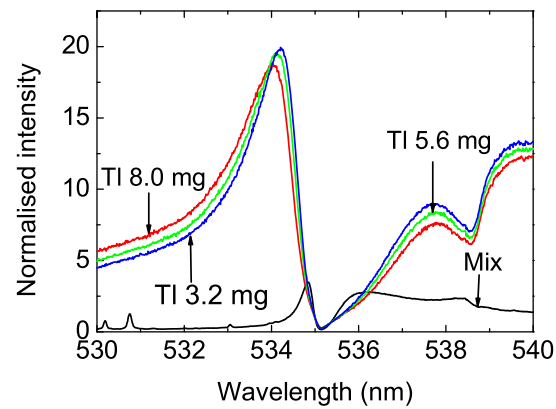


Figure 8.13: Spectra measured for three Tl lamps and one commercial CDM-T 70 W/830 lamp containing a mixture of NaI, DyI₃ and TlI. The intensity of the spectrum is normalised at 535 nm.

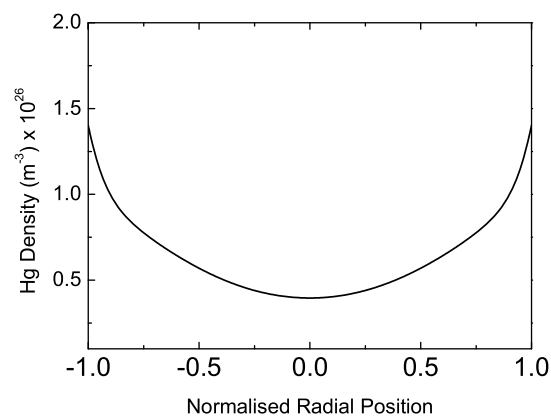


Figure 8.14: Density for the commercial CDM-T 70 W/830 lamp, determined from the mid-plane.

profile shape 1.6 %.

8.6 Acknowledgments

This research is sponsored by the Technologiestichting STW (project No. ETF 6093) and COST (project 529). The authors would like to thank M. van Grunsven and F. Vermeulen of Philips Lighting for supplying the lamps used in this study.

Bibliography

- [1] Lister G G, Lawler J E, Lapatovich W P and Godyak V A 2004 Rev. Mod. Phys. **76**, 541
- [2] Flesch P, *Light and light sources High intensity discharge lamps*, Springer-verlag, Berlin Heidelberg, 2006
- [3] Fischer E 1976 J. Appl. Phys. **47**, 2954
- [4] Zhu X 2005 Ph.D. thesis, Eindhoven University of Technology
- [5] Flikweert A J, Van Kemenade M, Nimalasuriya T, Haverlag M, Kroesen G M W and Stoffels W W 2006 J.Phys.D **39**, 1599
- [6] Flikweert A J, Nimalasuriya T, Groothuis C H J M, Kroesen G M W and Stoffels W W 2005, J. Appl. Phys. **98** 073301
- [7] Nimalasuriya T, Pupat N B M, Flikweert A J, Stoffels W W, Haverlag M and Van der Mullen J J A M 2006 J. Appl. Phys. **99** 053302 **see chapter 2**
- [8] Nimalasuriya T, Flikweert A J, Haverlag M, Kemps P C M, Kroesen G M W, Stoffels W W, Van der Mullen J J A M 2006 *J. Phys D: Appl Phys* **39** 2993 **see chapter 3**
- [9] Nimalasuriya T, Curry J J, Sansonetti C J, Ridderhof E J, Shastri S D, Flikweert A J, Stoffels W W, Haverlag M, Van der Mullen, J J A M 2007 J.Phys.D **40**, 2831 **see chapter 6**
- [10] Nimalasuriya T, Thubé G M, Flikweert A J, Haverlag M, Kroesen G M W, Stoffels W W, Van der Mullen 2007, J.Phys.D 2007 **40** 2839 **see chapter 4**
- [11] Stoffels W W, Baede A H F M, Van der Mullen J J A M, Haverlag M and Zissis G 2006 Meas. Sci. Technol. **17** N67
- [12] Cornelis R 2006, MSc Thesis, X-Ray Absorption measurements and measurement simulations on HID lamps, Eindhoven University of Technology
- [13] Denisova N, Haverlag M, Ridderhof E J, Nimalasuriya T, Van der Mullen J J A M, to be submitted
- [14] Nimalasuriya T, Zhu X, Ridderhof E J, Haverlag M, Denisova N, Stoffels W W and Van der Mullen, *submitted for publication in JPhysD*. **see chapter 7**
- [15] Bartels H Z 1950 Z. Phys. **127** 243
- [16] Karabourniotis D 1983 J. Phys D **16** 1267
- [17] Kettlitz M, Wendt M, Schneidenbach H and Krylova O 2007 J. Phys D **40**3829

- [18] Fohl T, Kramer J M and Lester J E 1993 J Appl Phys 73 46
- [19] Curry J J, Sakai M and Lawler J E 1998 J. Appl. Phys. **84**, 3066
- [20] Hansen P C, The L-curve and its use in the numerical treatment of inverse problems
- [21] Pretzler G, A New Method for Numerical Abel-Inversion, Z. Naturforsch. 46a, 1991, pages 639-641
- [22] Thermodynamic Database Philips Lighting
- [23] Van den Hoek W J, Van den Nieuwenhuizen H C M, Stormberg H P, *the estimation of additive densities in metal-halide arcs from self-reversed emission line contours*, (Philips Eindhoven 1982)
- [24] database for x-ray absorption cross-sections, <http://www.csrii.iit.edu/periodic-table.html>
- [25] Nimalasuriya T, Beks M L, Flikweert A J, Haverlag M, Stoffels W W, Kroesen G M W, Van der Mullen J J A M, *to be submitted to Special Edition of J.Phys D. see chapter 5*
- [26] Johnston C W 2003 PhD Thesis *Transport and equilibrium in molecular plasma's: the sulfur lamp* Eindhoven University of Technology.